L.I. Nyrkova, L.V. Goncharenko, S.O. Osadchuk, S. M. Prokopchuk, A.V. Klymenko, V.A. Kostin

Sress-corrosion cracking under cathodic protection of low alloy steel joints with high frequency weld and arc weld

E.O. Paton Electric Welding Institute of the National Academy of Sciences of Ukraine, Kyiv, Ukraine, lnyrkova@gmail.com

According to the results of complex electrochemical, corrosion-mechanical and fractographic studies, the existence of three potential regions, in which the stress-corrosion cracking (SCC) of 17G1S (17G1S-U) steel in the NS4 model soil electrolyte occurs by different mechanisms was established and experimentally confirmed: at potentials positively than -0.8 V – by the mechanism of local anodic dissolution, at potentials region from -0.8 V to -0.98 V – by the mixed mechanism, at potentials less than -0.98 V by hydrogen breaking mechanism. The susceptibility to SCC of high-frequency weld joints, estimated by the coefficient of K_S, in the potential range from the corrosion potential to -1.2 V increases (K_S increases from 1.1 to 1.8), which is less intense than for steel 17G1S/17G1S-U (K_S increases from 1.1 to 2.8), for arc weld joints – does not change much enough (K_S increases from 1.1 to 1.3). The validity of K_S coefficient introduced for the base metal for comparative assessment of the susceptibility to SCC of welded joints, is provided in case that there are no defects in the welds and SCC occurs on base metal.

Keywords: oil pipeline, low alloy steel, welded joints, slow strain rate method, voltammetry, metallography, fractography, stress-corrosion cracking.

Introduction

For production of pipes for oil and gas pipelines, high-frequency welding (HFW) and arc welding technologies are used. Many practical studies are devoted to studying the characteristics of fatigue failure, which, according to the authors [1-6], is one of the main requirements for pipeline integrity.

The work [7] analyzed the cause of the formation of penetrating defects in steel pipes and showed that their failure is due to unsatisfactory fusion of the edges because of relatively low heat annealing.

There are also data [8] that local heat treatment at 930ºC (additional to full heat treatment at 690ºC) of the area near the weld increases the resistance against crevice corrosion. It is shown that crevice corrosion is related to the microstructure and chemical composition of the weld. The study of the influence of welding regulations and heat treatment modes on mechanical properties and corrosion

resistance showed [9] that high-frequency welding followed by high-temperature annealing ensures the strength and corrosion properties of welded joints of pipes made of low-carbon, low-alloy steels at the level of the base metal. Studies of the tensile strength and impact toughness of both the base metal and weld joint of X52 steel pipes made by high-frequency welding [10] showed that both the base metal and the weld joint have an excellent balance between strength and impact viscosity But welded joints have a lower cyclic endurance due to the influence of surface defects than the base metal, which must be taken into account when evaluating the intensity of pipes.

There are data [11] that the susceptibility of the heat affected zone (HAZ) to stress-corrosion cracking of a welded joint made of X70 steel in a model soil electrolyte depends on two factors: the influence of the HAZ microstructure on electrochemical reactions and the effect of mechanical properties on the development of corrosion

cracking. Hydrogen reduction processes can be significantly facilitated in the HAZ region if the cathodic potential is positively than -1050 mV (relative to the silver chloride reference electrode, s.c.e.). However, if the cathode potential is negativele than -1050 mV cathodic current densities of different microstructures are near equal. At potentials -650 and -850 mV, stress-corrosion cracking most likely develops in the HAZ region, and at -1200 mV – both in the HAZ region and in the base metal region simultaneously.

Tests' results of X65 welded joint in model soil electrolyte demonstrated [12] that with an increasing the polarization current density, brittle fracture characteristics were observed. Heat treatment changes the microstructure of the steel, which leads to a change in the susceptibility to SCC: more hard steel with bainitic microstructure shows higher susceptibility to SCC than steel without heat treatment and normalization.

The improvement of the quality properties of pipes, welded by high-frequency welding in Ukraine was achieved due to the application of complex measures for significant technological improvement of the production of these pipes, which made it possible to expand the range of pipes manufactured for main gas and oil pipelines, taking into account the requirements of modern standards for their quality [13, 14].

From the given above short review, it follows that the corrosion and mechanical properties of welded joints obtained by various welding methods under conditions of cathodic polarization are insufficiently covered. Therefore, the purpose of the work is to compare and evaluate the susceptibility to corrosion cracking of welded joints obtained by high-frequency and arc welding.

I. Materials and test methods

The methods of potentiometry, voltammetry, tests at constant deformation, slow strain test method, optical microscopy and scanning electron microscopy were used

for research.

The solution is a model soil electrolyte NS4 such a composition, g/l:
0.122 + 0.483 $NaHCO_3$ + 0.181 $CaCl_2$ + 0.131 $MgSO_4$ [15].
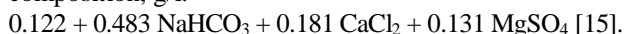
The research objects are the base metal and welded joints (made by high-frequency welding technology and arc method) of low-carbon steel 17G1C for pipelines. The research was conducted on samples of welded joints of 17GS-U steel, manufactured according to the technology used at the Novomoskovsk Pipe Plant, and on welded joints of pipes made of 17G1S steel, made by arc welding under flux. Samples were cut from pipes 530 mm in diameter and 10.0 mm thick made of 17G1S-U steel with high-frequency weld, and from pipes 1220 mm in diameter and 10.5 mm thick made from steel 17G1S with arc weld. The samples were made from pipe templates so that the weld seam was located in the middle of the samples, according to the sketch, Fig. 1.
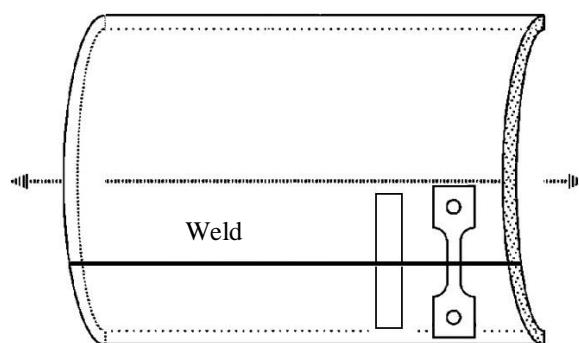

Fig. 1. Scheme of making samples from the pipe template.

Chemical composition and mechanical properties of steels under investigation are presented in Table 1 and in Table 2, respectively.

Electrochemical studies were performed on samples of welded joints with polished surface. A pressure cell was used to measure potentials and polarization curves. The

Table 1

Chemical composition of steels under investigation.

Steel grade	C	Mn	Si	S	P	Al	Ni	Mo	Ti	V	Nb	Cr
17G1S	0.16	1.32	0.47	0.023	0.016	-	0.06	-	-	-	-	0.04
HFW pipe of 17G1S-U steel	0.12	1.23	0.49	0.016	0.013	0.01	0.03		0.005		0.021	
TS 14-3-721	0.15-0.20	1.15-1.55	0.4-0.6	0.03	0.035	-	0.3	-	-			
Pipe with arc weld of 17G1S	0.147	1.30	0.49	0.022	0.016	0.095 (0.055)	0.08	0.011	0.001	-	-	-
GOST 5520	0.15-0.20	1.15-1.6	0.4-0.6	0.040	0.035	-	-	-	-	-	-	-
Base metal of 17G1S-U	0.12	1.23	0.49	0.016	0.013	0.01	0.03		0.005	0.03	0.021	

Table 2

Mechanical properties of steels under investigation.

Steel grade, sample characteristics	$\sigma_{0,2}$, MPa	σ_{yu}, MPa	δ, %
17Г1S sheet (according to GOST 5520)	345-355	510	23
HFW pipe from 17Г1S-U steel, base metal	400-430	560-580	-
17Г1S-U, HF weld joint	-	550-580	-
Arc weld pipe of 17G1S steel, base metal	522.2	646.3	-
Arc weld join of 17Г1S steel	-	616.8	-

potentials were measured relative to the silver chloride reference electrode (s.c.e.) using a PI-50-1.1 potentiostat. The polarization curves were recorded on the base metal and the weld seam of the welded joint samples in the potentiodynamic mode with a potential sweep speed of $5 \cdot 10^{-4}$ V/s. During the study of the mechanism of stress-corrosion cracking, the potential scan rate was $5 \cdot 10^{-4}$ V/s and 0.1 V/s.

Susceptibility to stress-corrosion cracking was studied by slow strain rate of the samples at 10^{-6} s^{-1} on the AIMA-5-1 tearing machine with full immersion in the NS4 solution. Flat samples of the MI-8 type [16] were used, the weld was placed in the middle of the specimen. Samples were investigated in the potentials ranging from the corrosion potential to -1.2 V.

Polished sections for metallographic studies were made according to standard methods. The microstructure was revealed by etching in 4% nitric acid in ethyl alcohol. Metallographic studies were carried out on NEOPHOT 21 microscope, digital images of the microstructure of the samples were obtained using a Sigeta digital camera. Grain score was determined according to DSTU 8972 [17].

The surfaces of the samples after stress-corrosion cracking were analyzed by scanning electron microscopy on JSM 840 electron microscope (JEOL, Japan) in the mode of secondary and backscattered electrons at an accelerating voltage of 20 kV and an electron beam current $(10^{-7}\text{-}10^{-10})$ A.

Electrolytic irrigation of steel was studied based on the improved methodology of GOST 9.915 [18]. The concentration of hydrogen penetrating back into the steel was calculated according to the formula:

$$J_{st} = \frac{I_{st}}{FS} = \frac{DC_0}{L},\qquad(1)$$

where J_{st} – the flow of hydrogen penetration into the surface layer of steel on the oxidized side of the membrane at steady state, mole/(m²·s);

I_{st} – current strength in the stationary regime of hydrogen penetration, A;

S – the area of the test sample from the side of the oxidation chamber, m²;

F – Faraday's constant, 96485 Kl/mole;

D – the diffusion coefficient of hydrogen, equal to $1{,}5 \cdot 10^{-5}$ cm²/s;

C_0 – hydrogen concentration in the surface layer of the steel membrane on the side of the hydrogenation chamber, mole/m³;

L – membrane thickness, m.

The current strength in the stationary mode of hydrogen penetration was calculated according to the equation:

$$I_{st} = I_{H_2} - I_{\text{b}},\qquad(2)$$

where I_{H_2}– the total amperage measured in the oxidation chamber, A; I_{b} – background current, A.

II. Experimental results and their discussion

2.1. Microstructure of the base metal and welds

The microstructure of base metal of 17G1S-U pipe is a mixture of fine-grained ferrite and pearlite with ferrite grains number 9-10 (Fig. 2, a). The banding of steel is characterized by a score of 4-5 on scale 3 (GOST 5640). The contamination of the base metal is local, in separate zones, mostly with slag inclusions, small globular oxides, extracted oxides, including near the fusion zone (Fig. 2, b). The microstructure of the metal in the near-seam area of the sample with a high-frequency seam is a typical fine-grained ferrite-pearlite mixture. The total width of this zone on the outer surface of the pipe is (19-23) mm, and on the inner surface - (10-13) mm. Based on the available experience, such a width of the local heat treatment zone is considered optimal, which ensures that its width is close in size from the inner and outer sides of the pipe.

The microstructure of the base metal of the 17G1S pipe steel is dispersed mixture of polygonal ferrite with the decomposition products of bainite and martensite. The share of the ferrite component does not exceed 30% (Fig. 3, a). Non-metallic inclusions are typical for steel of this class: linear oxides, plastic silicates, brittle and undeformed (including globular), sulfides and single aluminum nitrides.
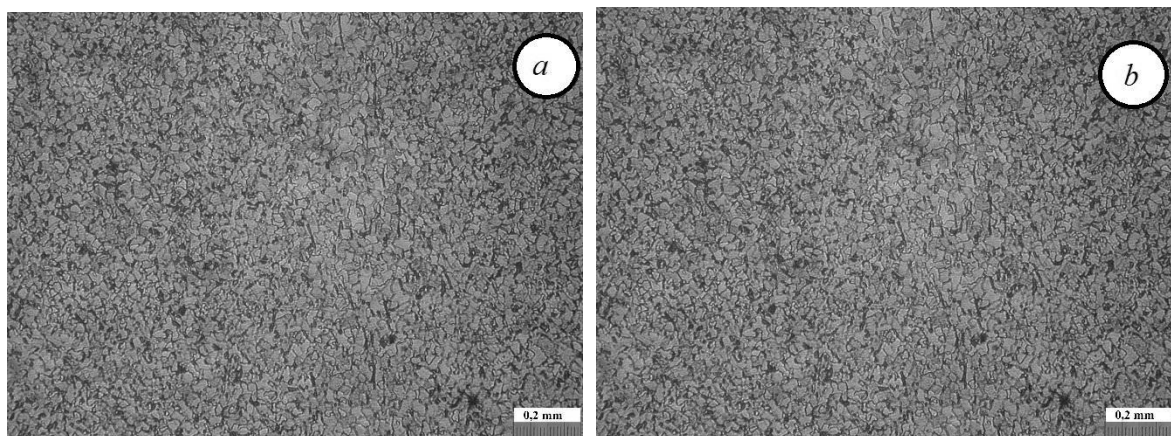

Fig. 2. Microstructure of the base metal (a) and metal of the high-frequency weld (b) of 17G1S-U steel pipe [19].

L.I. Nyrkova, L.V. Goncharenko, S.O. Osadchuk, S. M. Prokopchuk, A.V. Klymenko, V.A. Kostin
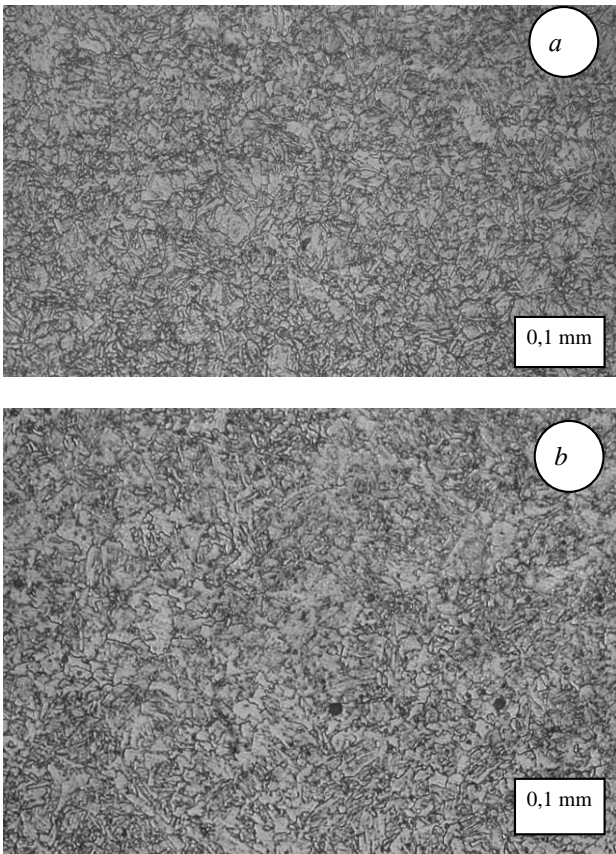
Fig. 3. Microstructure of the base metal of 17G1S steel (a) and the arc weld metal (b) of pipe [19].

The microstructure of the metal of the arc weld from the outside is a typical structure of a low-alloy metal after quenching and tempering and represents a dispersed ferrite-carbide mixture (of the sorbite type) with ferrite allocations (Fig. 3, b). Non-metallic inclusions in the metal of the arc weld in terms of morphology, number and size are characteristic of the metal of the welds made on steel of this class using acidic molten flux of the AN-60 type and are mainly globular silicon-manganese oxides.

2.2. Electrochemical properties of welded joints

Fig. 4 presents polarization curves of the base metal of steel 17G1S (17G1S-U) and welds, from which the electrochemical characteristics are determined, that given in the Table. 3.

Analyzing the electrochemical data, it was established that there is difference between the corrosion potentials of the base metal and welds, Tabl. 3: corrosion potentials of high-frequency weld and arc weld are negatively than the corrosion potentials of the base metal of 17G1S (17G1S-U) steel. The potential difference between the base metal and the high-frequency weld and the base metal and the arc weld is 14 and 16 mV, respectively, Table 3.

According to GOST 9.005 [20], such a potential difference does not represent a danger (a potential difference of more than 50 mV is considered dangerous for welded joints) and it can be expected that it will not lead to the predominant corrosion of a separate zone, in particular the weld.
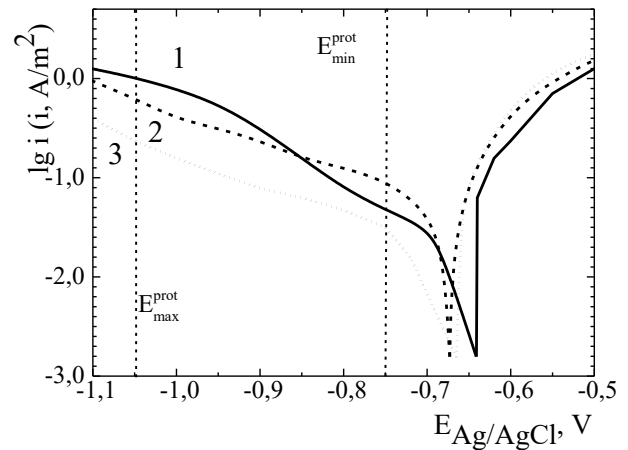
Fig. 4. Polarization curves of the base metal of 17G1S (17G1S-U)steel (1) and welds made by high-frequency welding technology (2) and arc welding technology (3).

The nature of the anodic and cathodic polarization curves of both the base metal and welds is the same. Anodic curves for welds are in the region of more negative potentials compared to the base metal. The currents of anodic dissolution of weld metal of all types of welded joints are practically the same in the region from the corrosion potential to 0.5 V, which indicates the similarity of their anodic behavior. Based on the values of the slopes of the anodic curves, it was established that the corrosion process in a neutral aqueous solution proceeds with diffusion control.

The value of the limit current of oxygen reduction on

Table 3.

Electrochemical characteristics of different zones of welded joints of 17G1S-U steel in 3% NaCl.

Zone of the welded joint	E_k, V	Electrochemical indicators of processes					
		anodic		cathodic			
		b_a, V	i, A/m²	i_d, A/m²	E_{H_2}, V	Cathodic currents, A/m², at polarization potentials, V	
						-0,75	-1,05
Base metal	-0.658	0.064	0.047	0.047	-0.79	0.048	0.97
High frequency weld	-0.683	0.066	0.185	0.160	-0.94	0.093	0.62
Arc weld	-0.674	0.049	0.062	0.053	-1.11	0.032	0.23
Notes. E_{cor} - corrosion potential; b_a - the slope of anode polarization curve; i - anode current density at potential of -0.64 V; i_d - the density of the limit diffusion current of oxygen reduction; E_{H_2} - the potential of hydrogen reduction.							

the base metal is 4 times less than on a weld made by high-frequency welding, and 1.3 times less than for an arc weld, table. 3. Since in the conditions of free access of oxygen in aqueous solutions, corrosion proceeds with diffusion control, larger currents of oxygen recovery on welds can contribute to the acceleration of the corrosion process in this potentials' area, which requires increased attention.

Hydrogen recovery potentials on all welds are approximately (8-32) mV negatively than on the base metal, Table. 3, which under certain influence of factors can create the conditions for preferential hydrogenation of the weld.

2.3. Corrosion and mechanical studies of pipe steel 17G1S (17G1S-U) and welded joints

Photographs of the fracture area of 17G1S-U steel samples and welded joints tested in air and in solution at different cathodic polarization potentials are presented in Fig. 5, sample destruction diagrams are presented are stated – in Fig. 6. From the analysis of the breaking diagrams in air (Fig. 6, curves 1, 3, 5) it can be seen that the rupture of welded samples occurs faster comparatively with the base metal. The breaking process of welded joints

is accompanied by smaller relative elongation, which is equal to 31% for the base metal, 20% and 24% for welded joints (Fig. 6, curves 1, 3, 5). The relative narrowing of the samples is 48%, 46% and 44.4%, respectively. The nature of the destruction is viscous holes, the holes have different depths and diameters, Fig. 7 (photo 1).

During the destruction of the samples in the NS4 solution under corrosion potential (Fig. 6, and curves 2, 4, 6), the rupture of the samples, both the base metal and the welded joints, occurs slightly faster compared to their destruction in air: it was noted the decreasing of indicators of relative narrowing to 43%, 36% and 41.3%, respectively; the relative elongation is within the range of data scatter, 31.42%, 17.1% and 17.6% (Fig. 6, a, curves 2, 4, 6). The break line of the base metal and the high-frequency connection made of 17G1S-U steel is smooth, break line of the arc connection is wavy, polyline, Fig. 5. On the surface of the fractures, there are signs of viscous failure, the enlargement of holes is visible, Fig. 7 (photo 2). The tendency to corrosion cracking is low, the K_S coefficient is 1.1, 1.28 and 1.1 for the base metal, high-frequency and arc connections, Fig. 8 (curves 1-3).

In air

| S=30,92 mm^2 | S=16,2 mm^2 | S=16,7mm^2 |

E$_{cor}$

| S=31,42 mm^2 | S=19,2 mm^2 | S=17,6 mm^2 |

E$_{pol}$ = -0,75 V

| S=32,81 mm^2 | S=19,7 mm^2 | S=17,4 mm^2 |

E$_{pol}$ = -0,95 V

| S=34,5 mm^2 | S=21,1 mm^2 | S=18,8 mm^2 |

E$_{pol}$ = -1,05 V

| S=29,2 mm^2 | S=20,9 mm^2 | S=18,7 mm^2 |

E$_{pol}$ = -1,2 V

| S=27,0 mm^2 | S=21,3 mm^2 | S=19,2 mm^2 |

a   *b*   *c*
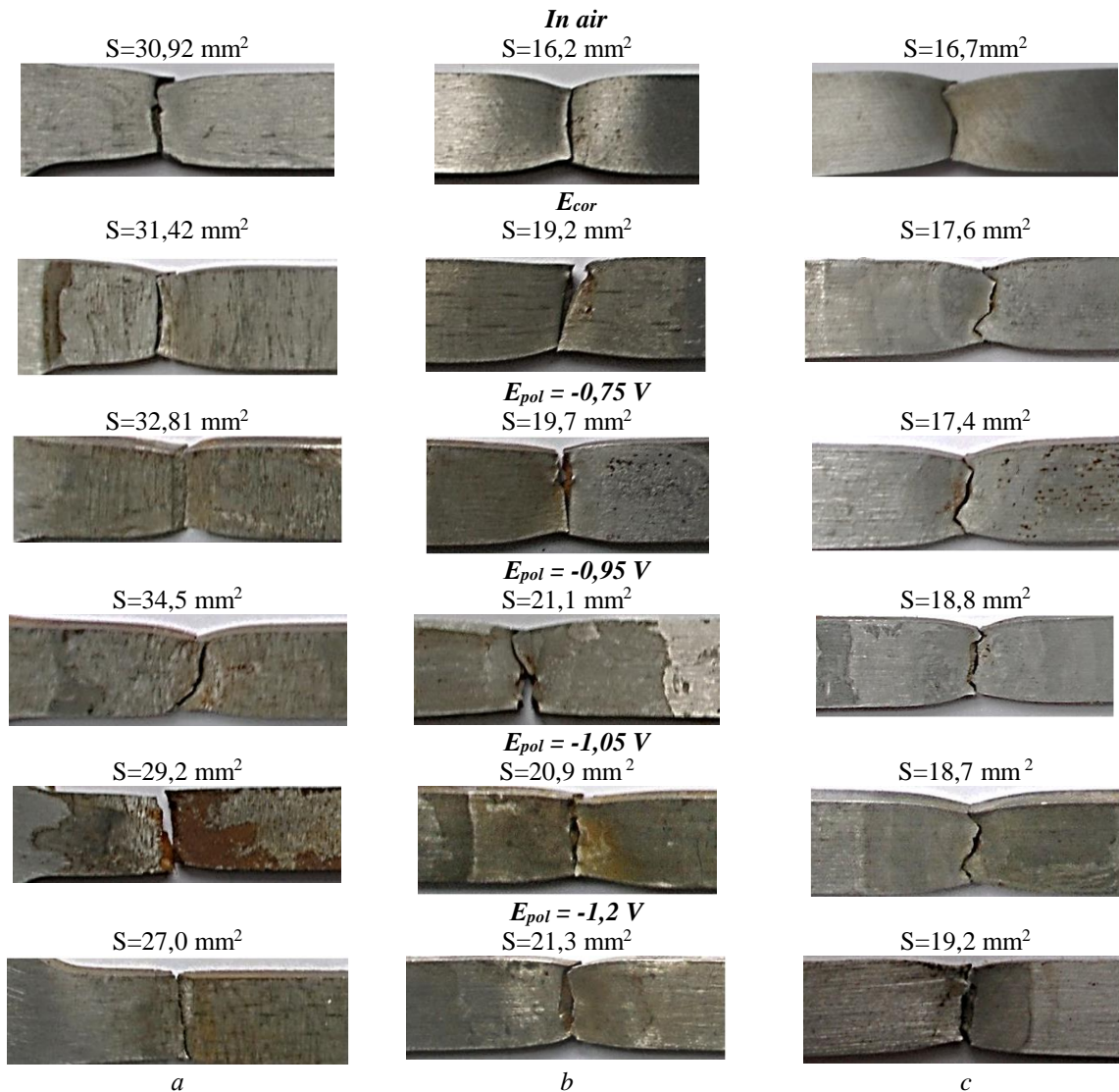
Fig. 5. View of the fracture area of the base metal (a) of 17G1S steel (17G1S-U) and welded joints made by high-frequency welding (b) and arc (c) welding after mechanical tests in air and corrosion-mechanical tests in model soil electrolyte NS4 at different potentials.
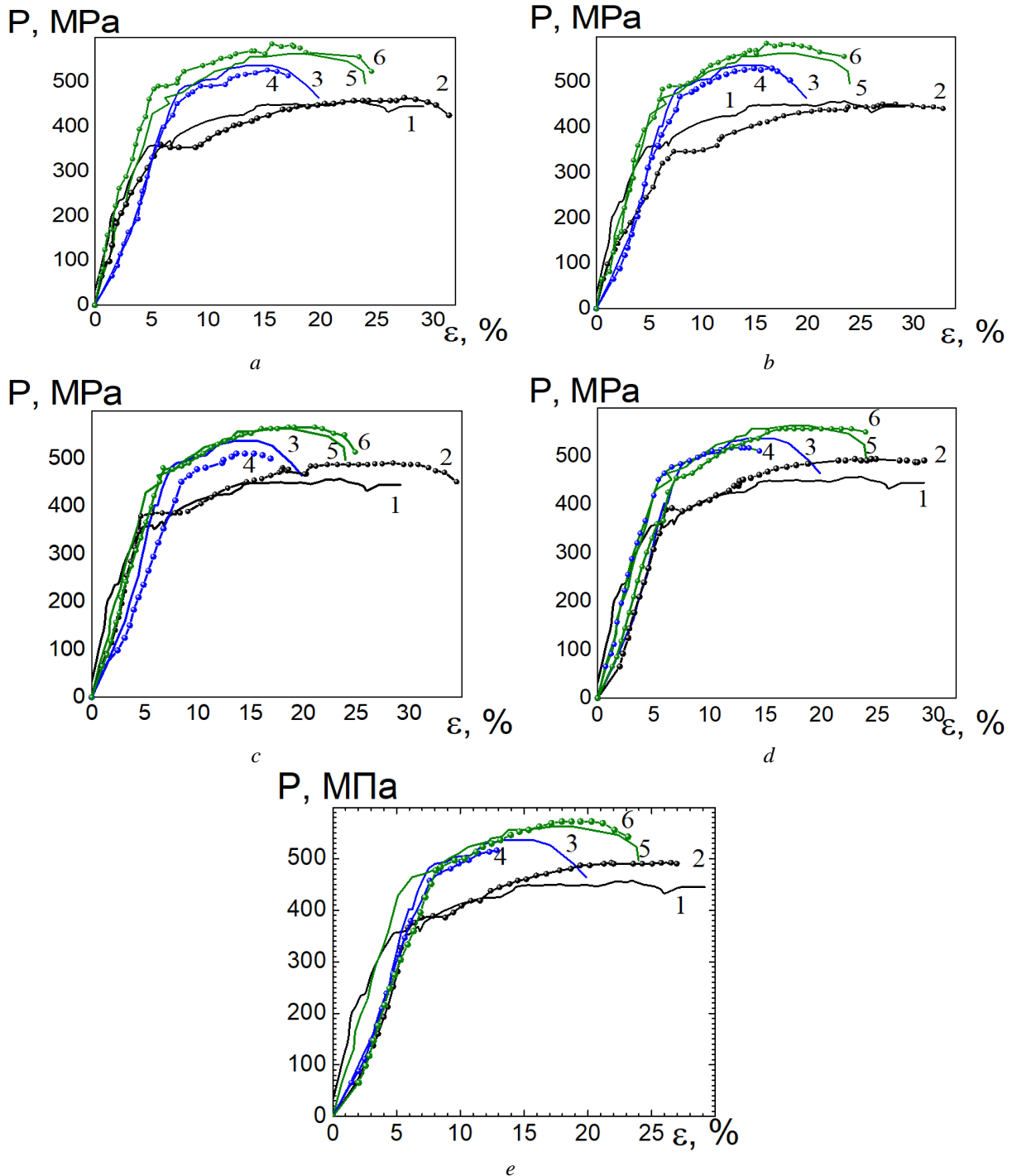
Fig. 6. Breaking diagrams of samples of base metal and welded joints made of 17G1S steel (17G1S-U) in air and in NS4 solution under different conditions: 1, 2 – base metal; 3, 4 – high-frequency welded joint; 5, 6 – arc welded joint 1, 3, 5 – in air; 2, 4, 6 – at corrosion potential or at cathodic polarization potential, a – E_{cor}; b – E_{pol} = -0.750 V; c – E_{pol} = -0.950 V; d – E_{pol} = -1.05 V; e – E_{pol} = -1.2 V.

Under the minimum protective potential -0.75 V in the NS4 solution, Fig. 6, b (curves 2, 4, 6) the relative elongation indicators for all samples were within the range of the data dispersion and were equal for the base metal, high-frequency joint and arc joint, respectively, 32.81%, 18.3% and 23.5%; the relative shrinkage decreased to 42%, 34% (most strongly compared to the relative shrinkage of samples in air) and 42.1%. The break line of the base metal remained smooth; the fragments of polyline appeared in the fracture line of the welded joints, Fig. 5. On all samples, the characteristic shrinkage near the place

of rupture remains. On the surfaces of the fractures, there are signs of mostly viscous failure, but flat areas appear, Fig. 7 (photo 3).

The susceptibility to stress-corrosion cracking, estimated by the K_S coefficient, is equal to 1.1, 1.34 and 1.1 for the base metal, high-frequency and arc connections, respectively, Fig. 8.

At protective potential in the normalized range -0.95 V in the NS4 solution, Fig. 6, c (curves 2, 4, 6) the value of relative elongation indicators for all samples were within the range of the data scatter and for the base metal,
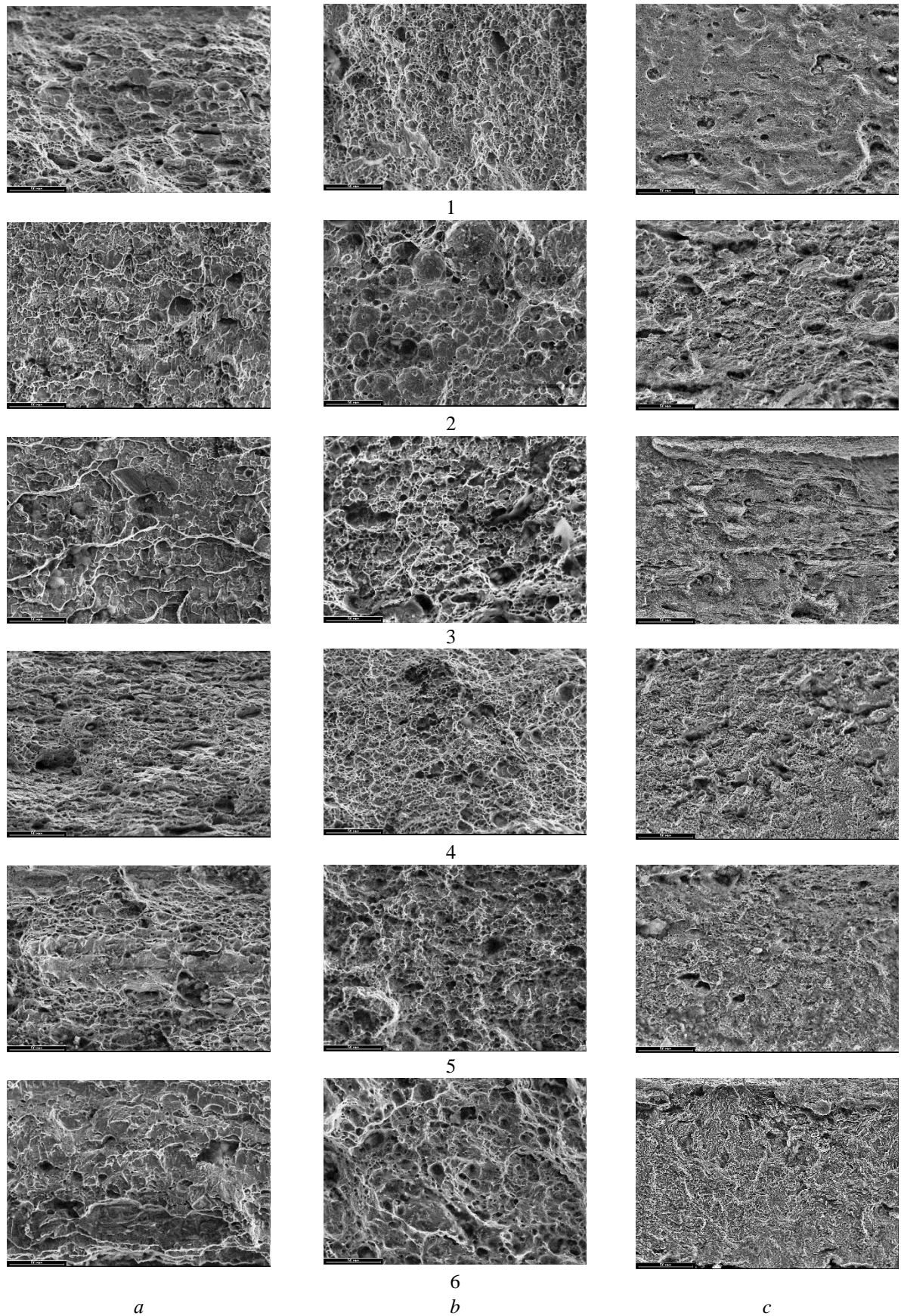
Fig. 7. Fractograms of fracture surfaces of base metal samples (a) made of 17G1C-U steel with high-frequency weld (b) and arc weld (c) in air and in NS4 solution under different conditions: 1 – in air; 2 – at corrosion potential; at cathode potentials, 3 – -0.75 V, 4 – -0.95 V, 5 – -1.05 V, 6 – -1.2 V.
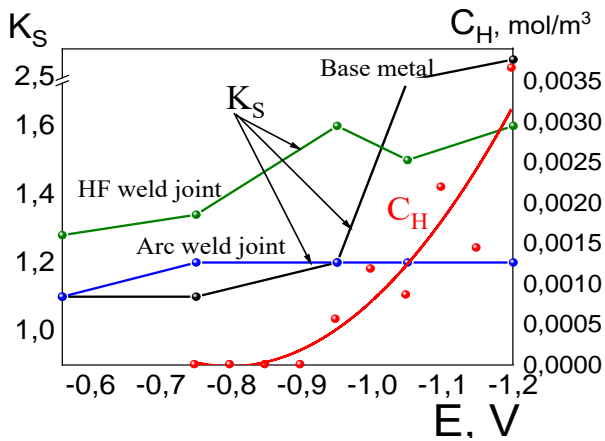
Fig. 8. Change in susceptibility to stress-corrosion cracking, estimated by the K_S coefficient and the concentration of hydrogen, penetrating into 17G1S-U steel, from the potential.

high-frequency and arc connections were equal, respectively to 34.5%, 16.9% and 24.9%; the relative narrowing for the base metal and the arc joint decreased to 39.7% and 37.4%, and little changed for the high-frequency joint at 29.7%. The fracture line of all samples near the break site is fractured, to a greater or lesser extent, there is a retraction characteristic of viscous fracture, Fig. 5. On the fracture surfaces, the proportion of flat areas of fracture increases and the proportion of hole fracture decreases. Fig. 7 (photo 4). The coefficient of susceptibility to stress-corrosion cracking was equal to 1.2, 1.6 and 1.2, respectively (Fig. 8).

During tests at the maximum protective potential - 1.05 V in NS4 solution (Fig. 6, c, curves 2, 4, 6), the relative elongation indicators for all samples were within the range of the data dispersion and were composed for the base metal, high-frequency and arc connections 29.16%, 4.5% and 23.3%, respectively; but the relative narrowing for these samples decreased to 26.3%, 30.3% and 37.8%. The retraction of all samples is noticeably less than in air, the rupture line is broken, Fig. 5. On the fracture surfaces, the share of flat fracture areas increases and the share of dimples decreases, Fig. 6 (photo 5). K_S coefficient is equal to 1.8, 1.5 and 1.2, that is, the main metal has the greatest tendency to stress-corrosion cracking, Fig. 8. So, with the shift of the potential from the minimum -0.75 V to the maximum protective -1.05 V, the susceptibility to brittle failure increased for the base metal of the 17G1S-U steel, less for the high-frequency joint, and slightly increased for the arc joint.

At the potential greater in absolute value than the maximum protective one, -1.2 V, Fig. 6, d (curves 2, 4, 6) decreasing both in the relative elongation of the samples of the base metal, high-frequency weld joint and arc connection through the rupture to 27, 12.9 and 23.1%, and the relative contraction to 17%, 29% and 36.1%, respectively is observed. The rupture of all samples occurred practically without plastic deformation, their shrinkage is noticeably less than in air, the rupture line is broken, Fig. 5. On fracture surfaces, the share of flat areas of destruction prevails, the share of dimples decreases, Fig. 7 (photo 5). The regularity of changes in susceptibility to stress-corrosion cracking is the same as with the

maximum protective potential: K_S is 2.8, 1.6 and 1.2, i.e. the base metal exhibits the greatest susceptibility to stress-corrosion cracking.

Comparing the results of determining of hydrogen concentration that penetrates through the 17G1S steel (17G1S-U) during cathodic polarization in the NS4 solution, it was established that hydrogen penetration begins at the potential of -0.95 V (its content in steel is equal to 0.00056 mole/m³), and at the maximum protective potential reaches a value of 0.00086 mole/m³. Similarly, the propensity of the base metal of 17G1S-U steel to stress-corrosion cracking increases. The susceptibility to stress-corrosion cracking of high-frequency welded joint in the investigated potentials range increases, but less intensively than for the base metal. For an arc connection, the susceptibility to stress-corrosion cracking is almost the same over the entire potential range.

Decreasing in the relative narrowing of the samples during the tests indicates that under influence of corrosive environment and cathodic polarization, slow embrittlement of the near-surface layer occurs, which contributes to the development of brittle fracture.

It should be noted that in the absence of defects in welds (non-weldings, pores, accumulation of non-metallic inclusions, etc.), the destruction of welded joints occurs on the base metal. This confirms the legality of using the introduced K_S coefficient for comparative evaluation of susceptibility to corrosion cracking of welded joints. The tendency to corrosion cracking, estimated by the K_S coefficient, for the base metal and for the high-frequency welded joint increases most intensively when the cathodic potential approaches the maximum protective potential and above it, for the arc welding joints the K_S coefficient remains almost the same both in the normalized range of protective potentials and at the potential, greater than the maximum protective one.

Thus, with the displacement of the potential from the minimum to the maximum protection, the susceptibility to brittle failure increased for the base metal, less for the high-frequency welded joint, and slightly increased for the arc welded joint.

Conclusions

1. According to the results of complex of electrochemical, corrosion and mechanical and fractographic studies, the existence of three potential regions was established and experimentally confirmed, in which corrosion cracking of 17G1S steel (17G1S-U) in the NS4 soil electrolyte occurs by different mechanisms:

- in the region of potentials more positive than -0.8 V, stress-corrosion cracking proceeds by the mechanism of local anodic dissolution, hydrogen penetration through the steel does not occur, the values of the coefficient vary from 1.1 to 1.16, the morphology of the fracture surface is viscous;

- in the range of potentials from -0.8 V to -0.98 V, cracking occurs according to the mechanisms of local anodic dissolution and hydrogen cracking: the concentration of hydrogen, capable to penetrate through the steel membrane, increases, the coefficient of susceptibility to stress-corrosion cracking K_S increases

from 1.16 to 1 ,58, areas of brittle fracture appear in the fracture morphology;

- in the region of potentials more negative than -0.98 V, hydrogen cracking prevails: the concentration of hydrogen penetrating the steel and the coefficient of susceptibility to corrosion cracking from 1.56 to 4.38 increase intensively, which correlates with an increasing in the proportion of brittle areas on the surface destruction.

2. Welded joints made of 17G1S steel, obtained by high-frequency welding and arc welding, in the NS4 soil electrolyte under cathodic polarization have the following patterns:

- the susceptibility to stress-corrosion cracking of the high-frequency connection in the range from the corrosion potential to -1.2 V increases (from 1.1 to 1.8) less intensively than for the base metal (from 1.1 to 2.8), for arc joint it does not change much (from 1.1 to 1.3);

- the most significant susceptibility to stress-corrosion cracking for the base metal and for the high-frequency welded joint made of 17G1S steel increases when the cathodic polarization potential approaches the maximum protective potential -1.05 V and above it, for the arc joint susceptibility to stress-corrosion cracking remains almost the same as in the normalized range of protective potentials, as well as at a potential greater than the maximum protective potential.

3. The legality of using the corrosion cracking susceptibility coefficient K_S, introduced for the base metal, for the comparative evaluation of the corrosion cracking susceptibility of welded joints has been established, since in the absence of defects in the welds (non-weldings, pores, accumulation of non-metallic inclusions, etc.) the destruction of welded joints connections take place on the base metal.

Nyrkova L.I. – Doctor of technical sciences, Head of the Department of welding of gas and oil pipelines;
Goncharenko L. V. – Junior researcher of Department welding of gas and oil pipelines;
Osadchuk S.O. – PhD in technical sciences, Researcher of the Department of welding of gas and oil pipelines;
Prokopchuk S.M. – PhD student of the Department of welding of gas and oil pipelines;
Klymenko A. V. – PhD in technical sciences, Senior Researcher of the Department of gas and oil welding;
Kostin V. A. – Doctor of technical sciences, Leading Researcher of the Department of physico-chemical studies of materials.

[1] B. Pinheiro, I. Pasqualino, S. Cunha, Fatigue life assessment of damaged pipelines under cyclic internal pressure: pipelines with longitudinal and transverse plain dents, International Journal of Fatigue, 68, 38 (2014); https://doi.org/10.1016/j.ijfatigue.2014.06.003.

[2] J. X. Zhao, W. X. Chen, K. Chevil et al, Effect of pressure sampling methods on pipeline integrity analysis. Journal of Pipeline Systems Engineering and Practice, 8 (4), Article 04017016 (2017).

[3] M. A. Neves Beltrão, E. M. Castrodeza, F. L. Bastian, Fatigue crack propagation in API 5L X-70 pipeline steel longitudinal welded joints under constant and variable amplitudes, Fatigue and Fracture of Engineering Materials and Structures, 34 (5), 321 (2011); https://doi.org/10.1111/j.1460-2695.2010.01521.x.

[4] O. Fatoba, R. Akid, Low cycle fatigue behaviour of API 5L X65 pipeline steel at room temperature, Procedia Engineering. 2014. 74, 279 (2014); https://doi.org/10.1016/j.proeng.2014.06.263.

[5] J. C. R. Pereira, A. M. P. de Jesus, A. A. Fernandes, G. Varelis, Monotonic, low-cycle fatigue, and ultralow-cycle fatigue behaviors of the X52, X60, and X65 piping steel grades, Journal of Pressure Vessel Technology, 138 (3), Article 031403 (2016); https://doi.org/10.1115/1.4032277.

[6] C. Taylor, S. Das, L. Collins, M. Rashid, Fatigue crack growth at electrical resistance welding seam of API 5L X-70 steel line pipe at varied orientations. Journal of Offshore Mechanics and Arctic Engineering, 139 (3), article 031401 (2017); https://doi.org/10.1115/1.4035385.

[7] B. Y. Lee, S. Lee, Studies on the microstructure and corrosion characteristics of electrical resistance welded steel, Advances in nondestructive evaluation, 270-273, 2327 (2004); https://doi.org/10.4028/www.scientific.net/KEM.270-273.2327.

[8] Z. Bi, R. Wang, X. Jing, Grooving corrosion of oil coiled tubes manufactured by electrical resistance welding, Corrosion Science, 57, 67 (2012); https://doi.org/10.1016/j.corsci.2011.12.033.

[9] L. M. Vyboishchik, A. V. Ioffe, Formation of structure and properties in welded joints of oil line pipes, Metal science and heat treatment. 2013. 54 (9-10), 535 (2013); https://doi.org/10.1007/s11041-013-9544-5.

[10] P. Tian, K. Xu, G. Lu, G. Qiao, B. Liao, Evaluation of the mechanical properties of the X52 high frequency electric resistance welding pipes, International Journal of Pressure Vessels and Piping. 2018. 165, 59 (2018); https://doi.org/10.1016/j.ijpvp.2018.06.006.

[11] Z. Y. Liu, C. W. Du, C. Li, F. M. Wang, X. G. Li, Stress Corrosion Cracking of Welded API X70 Pipeline Steel in Simulated Underground Water, Journal of Materials Engineering and Performance, 22, 2550 (2013); https://doi.org/10.1007/s11665-013-0575-2.

[12] HongxiaWanCuiwei, Du Zhiyong Liu, Dongdong Song Xiaogang Li, The effect of hydrogen on stress corrosion behavior of X65 steel welded joint in simulated deep sea environment, Ocean Engineering, 114 (1), 216 (2016); https://doi.org/10.1016/j.oceaneng.2016.01.020.

[13] Yu. N. Antipov, E. V. Dmitrenko, A. A. Kovalenko, S. A. Goryanoy, A. A. Rybakov, S. E. Semenov, T. N. Filipchuk, Improvement of operational reliability of oil and gas pipelines manufactured by the method high-frequency welding, Strength Problems, 5, 147 (2009).

[14] Yu. N. Antipov, E. V. Dmitrenko, A. A. Kovalenko, S. A. Goryanoy, A. A. Rybakov, S. E. Semenov, T. N. Filipchuk PJSC "Interpipe NMTW", Automatic welding. 2014. 3, 43 (2014).

[15] R. Antunes de Sena, I. Napoleão Bastos, G. Mendes Plat, Theoretical and Experimental Aspects of the Corrosivity of Simulated Soil Solutions, International Scholarly Research Notices, article ID 103715, 6 pages, (2012).

[16] L.I. Nyrkova, P.E. Lisovyi, L.V. Goncharenko, S.O. Osadchuk, V.A. Kostin, A.V. Klymenko, Regularities of Stress-Corrosion Cracking of Pipe Steel 09G2S at Cathodic Polarization in a Model Soil Environment, Physics and chemistry of solid state, 22 (4), 828 (2021); https://doi.org/10.15330/pcss.22.4.

[17] ДСТУ 8972:2019 Steel and alloys. Methods for detection and determination of grain size

[18] ГОСТ 9.915-2010 Unified system of corrosion and ageing protection. Metals, alloys, coatings, products. Test methods of hydrogen embrittlement.

[19] L. Nyrkova, S. Prokopchuk, S. Osadchuk, L. Goncharenko, Stress corrosion of welded joints of pipeline steel obtained by various welding methods, Physico-chemical mechanics of materials, Special issue 13, 83 (2020).

[20] ГОСТ 9.005-72 Unified system of corrosion and ageing protection. Metals, alloys, metallic and non-metallic coatings. Permissible and impermissible contacts with metals and non-metals.

Л.І. Ниркова, Л.В. Гончаренко, С.О. Осадчук, С.М. Прокопчук, А.В. Клименко, В.А. Костін

Корозійне розтріскування зварних з'єднань труб з низьколегованої сталі з високочастотним і дуговим швами в умовах катодного захисту

Інститут електрозварювання ім. Є.О. Патона НАН України, Київ, Україна, lnyrkova@gmail.com

За результатами комплексу електрохімічних, корозійно-механічних та фрактографічних досліджень встановлено та експериментально підтверджено існування трьох областей потенціалів, в яких корозійне розтріскування сталі 17Г1С (17Г1С-У) у модельному ґрунтовому електроліті NS4, відбувається за різними механізмами: за потенціалів позитивніших -0,8 В за механізмом локального анодного розчинення, від -0,8 В до -0,98 В – за змішаним механізмом, за потенціалів від'ємніше -0,98 В за водневим механізмом. Схильність до корозійного розтріскування високочастотного з'єднання, оцінена за коефіцієнтом K_S, в діапазоні від потенціалів від потенціалу корозії до -1,2 В зростає (K_S зростає від 1,1 до 1,8), що менш інтенсивно, ніж для сталі 17Г1С/17Г1С-У (K_S зростає від 1,1 до 2,8), для дугового – змінюється не сильно (K_S зростає від 1,1 до 1,3). Встановлено правомірність застосування коефіцієнту K_S, введеного для основного металу, для порівняльного оцінювання схильності до корозійного розтріскування зварних з'єднань, за умови відсутності у зварних швах дефектів.

Ключові слова: нафтопровід, низьколегована сталь, зварні з'єднання, деформація з малою швидкістю, вольтамперометрія, металографія, фрактографія, стрес-корозійне розтріскування.